

Optical Caustics in the Near Field from Liquid Drops

Author(s): J. F. Nye

Source: *Proceedings of the Royal Society of London. Series A, Mathematical and Physical Sciences*, Vol. 361, No. 1704 (May 3, 1978), pp. 21-41

Published by: Royal Society

Stable URL: <http://www.jstor.org/stable/79630>

Accessed: 24-11-2017 16:05 UTC

JSTOR is a not-for-profit service that helps scholars, researchers, and students discover, use, and build upon a wide range of content in a trusted digital archive. We use information technology and tools to increase productivity and facilitate new forms of scholarship. For more information about JSTOR, please contact support@jstor.org.

Your use of the JSTOR archive indicates your acceptance of the Terms & Conditions of Use, available at <http://about.jstor.org/terms>



Royal Society is collaborating with JSTOR to digitize, preserve and extend access to *Proceedings of the Royal Society of London. Series A, Mathematical and Physical Sciences*

JSTOR

Optical caustics in the near field from liquid drops

By J. F. NYE, F.R.S.

*H.H. Wills Physics Laboratory, University of Bristol,
Tyndall Avenue, Bristol BS8 1TL, U.K.*

(Received 10 August 1977)

[Plates 1–8]

When light passes through a small irregular droplet of water on a glass surface the envelopes of the refracted rays form a system of caustic surfaces. The caustics have been examined experimentally, and interpreted theoretically with the aid of Thom's theorem. The main feature of interest is a unique plane of focus which contains typically several tens of elliptic umbilic catastrophes. These unfold and interact by beak-to-beak events and swallowtail catastrophes to give the many-cusped figures observed close to the drop and in the far field. The primary generic events produced by an irregular drop are analysed by considering them as the unfoldings of a symmetrical case having four control parameters and containing two elliptic umbilics and two butterfly catastrophes.

1. INTRODUCTION

An irregular water drop resting on an inhomogeneously dirty glass surface acts as an imperfect lens. For example, the rays from a distant point source of light, after passing through such a drop, come to a focus not at a point, but on a system of caustics which are the envelopes of the rays. In a recent paper, showing how Thom's theorem on the singularities of mappings may be used to solve a variety of problems in wave physics, Berry (1976) used the irregular droplet lens as a simple but instructive example. The droplet produces a perturbed plane wavefront and Berry was concerned in the first instance with the caustics produced by the rays in the far field. In this paper we examine the near field.

Essentially we are concerned with the surface of centres (loci of the centres of curvature) of a wavefront. However, we do not discuss the general problem. The special case where the wavefront is restricted by the condition (from the surface tension of the droplet) that the sum of its principal curvatures is everywhere constant is sufficiently interesting for detailed discussion. Moreover, because such wavefronts are readily produced by passing light through water droplets their caustic patterns are easy to study experimentally.

2. PRELIMINARY THEORY

We first recall the result that the caustics produced by a wavefront, in the limit of geometrical optics, fall into Thom's classification. Although the result is true for a general wavefront, we confine ourselves here to the case where the slope of the wavefront is everywhere small. Let $\mathbf{r} = (x, y)$ be a position vector in the plane $z = 0$ (figure 1a) and let the wave front W be given by its height $f(\mathbf{r})$ above this plane, with $|\nabla f| \ll 1$. The position of a general point P in the space above the wavefront may be specified by its height Z and the vector $\mathbf{R} = (X, Y)$. We shall assume that $Z \gg f$. Consider the generating function

$$\phi = f(\mathbf{r}) - \{(\mathbf{R} - \mathbf{r})^2/2Z\}. \quad (1)$$

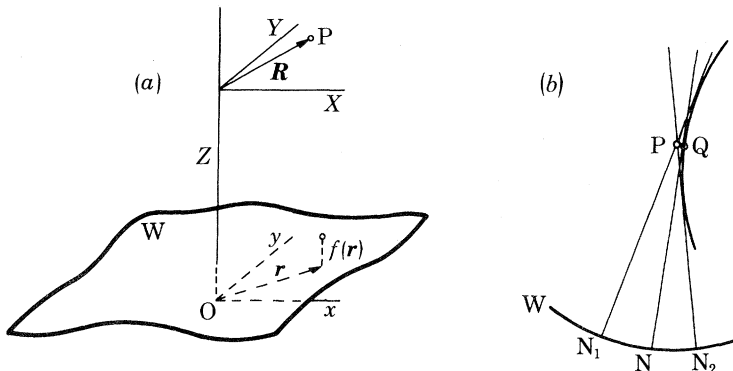


FIGURE 1. (a) Notation for the wavefront W and the point P in the space above it. (b) The point P above the wavefront W lies on the normals from N_1 and N_2 . When P moves to Q , N_1 and N_2 coalesce at N . Q is a centre of curvature and lies on the envelope of the rays, a caustic. This is the most elementary type of focusing.

Keeping (X, Y, Z) fixed and varying (x, y) , the condition for ϕ to be stationary is

$$\nabla_{\mathbf{r}} \phi = 0, \quad (2)$$

which implies

$$\nabla f(\mathbf{r}) = (\mathbf{r} - \mathbf{R})/Z.$$

Since $Z \gg f$ this equation is satisfied on a normal from P to the wavefront, that is to say, on a ray through P . Thus ϕ given by (1) generates, through (2), the rays whose envelopes, in the approximation $Z \gg f$, we wish to consider. The rays give a mapping from the three-dimensional space above the wavefront (control space) into the two-dimensional space (state space) of the wavefront itself. Each point P in control space can be associated by (2) with several separated points, the feet of the normals, in state space (figure 1b). Singularities arise when the point in control space is moved to a place where two or more of its associated points in state space come together; this represents focusing, and the point in control space then lies on the envelope of the rays, a caustic. Thom's theorem (see, for example, Berry

1976) applies to gradient mappings such as that given by (2) and allows us to state that the only caustics that will normally occur are the elementary catastrophes of co-dimension (dimension of control space) less than or equal to 3, namely, the fold, cusp, swallowtail, elliptic umbilic and hyperbolic umbilic. Any other type of focus is structurally unstable, in the sense that a small general perturbation of the wavefront will cause it to break up into an array of these elementary catastrophes.

The physical meaning of the generating function (1) may be seen by noting that the distance l between a general point in the wavefront (\mathbf{r}, f) and the general point $\mathbf{P} = (\mathbf{R}, Z)$ is given by

$$l^2 = (\mathbf{R} - \mathbf{r})^2 + (Z - f)^2.$$

Then

$$\phi \simeq (Z^2 - l^2)/2Z \quad (f \ll Z).$$

Thus, for fixed \mathbf{P} , the condition (2) for ϕ to be stationary is the same as the condition for l to be stationary, and this in turn is the property of a ray though \mathbf{P} .

Specifically, we are concerned with the wavefronts produced from a distant point source by liquid droplet lenses whose slopes are small and which are small enough in their vertical dimension for gravity to have negligible effect on their shape. A water droplet a few millimetres in size resting on a horizontal and moderately clean glass plate satisfies these conditions well enough.

Let the top surface of the glass be at $z = 0$. If $h(x, y)$ is the thickness of the drop, the height of the wavefront, W , immediately above the drop is

$$f(x, y) = (1 - n) h(x, y) + \text{a small constant}, \quad (3)$$

where n is the refractive index of water. Because the excess internal pressure p of the drop is uniform the surface tension γ causes $f(x, y)$ to satisfy the equation

$$\frac{\partial^2 f}{\partial x^2} + \frac{\partial^2 f}{\partial y^2} = \frac{(n-1)p}{\gamma} = C, \quad \text{say}, \quad (4)$$

C being a positive constant.

If $C_1(\mathbf{r})$ and $C_2(\mathbf{r})$ are the two principal curvatures of W at $\mathbf{r} = (x, y)$, ($C_1 \geq C_2$), we have

$$C = C_1(\mathbf{r}) + C_2(\mathbf{r}). \quad (5)$$

The Gaussian curvature is the product $C_1(\mathbf{r})C_2(\mathbf{r})$ and we may define the curvature difference $D(\mathbf{r})$ by

$$D(\mathbf{r}) = C_1(\mathbf{r}) - C_2(\mathbf{r}). \quad (6)$$

In a general wavefront the caustic surfaces are the loci of its centres of curvature, and therefore on a screen a given height above the wavefront the caustic curves originate from contours on the wavefront of constant C_1 and constant C_2 . But in our case, where C_1 and C_2 have a fixed relation, namely (5), the contour maps of each of the four quantities C_1 , C_2 , D and C_1C_2 are identical; only the labels on the individual contours are different.

It is convenient to choose from these quantities the curvature difference D , and to visualize its distribution over the drop as represented by the height of a landscape

(figure 2). D is essentially positive, and its landscape has certain interesting general features (appendix A). First, there are a number of minima which are all at zero height; these are the umbilic points where the wavefront surface W is locally spherical. These minima of D are locally conical, and they are the only minima. The only other stationary points are saddles; there are no maxima. The total curvature of the D -landscape (the sum of its principal curvatures) is never negative, a condition involving the fourth derivatives of the surface W . Thus the D -landscape may be pictured as a bowl in which are contained a number of conical minima all at zero level, these minima being separated by saddle points at varying levels; but, if one climbs up from a saddle point, one never finds a maximum before being stopped either by the edge of the drop or by the breakdown of the small-slope approximation.

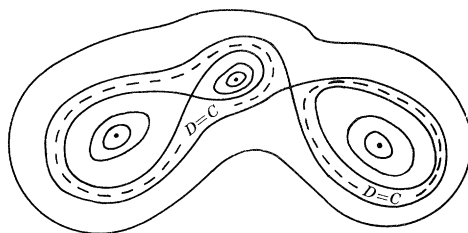


FIGURE 2. Contours of the D -landscape.

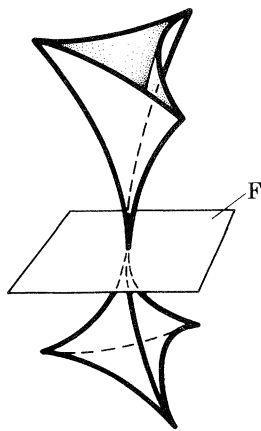


FIGURE 3. Caustics at an elliptic umbilic focus.

The contour $D = C$ has the special property that on it $C_2 = 0$; thus this is the line on the wavefront which is responsible for the directional caustic in the far field, as discussed by Berry (1976) (it is the line \mathcal{L} in fig. 2 of his paper, where the Gaussian curvature $C_1 C_2$ of W vanishes). At an umbilic point $D = 0$, $C_1 = C_2 = \frac{1}{2}C$, and the rays focus at a height $\rho = 2C^{-1}$ above the wavefront W which we call the

focusing level F. It is important to notice that all the umbilic points focus at this same level. Let D_1 be a value of D less than C. The D_1 contour gives a caustic at two levels, u_1 and u_2 say, below and above level F: $u_1 = C_1^{-1}$ and $u_2 = C_2^{-1}$. By equation (5),

$$\frac{1}{u_1} + \frac{1}{u_2} = \frac{2}{\rho}. \quad (7)$$

We call these levels conjugate by analogy with the object-image relation for a spherical concave mirror of radius ρ .

The foci from the zeros of D are elliptic umbilics (appendix B), sketched in figure 3. One has to imagine a set of these all lying at the same level F and opening out above and below this focusing level, with the caustics at conjugate levels coming from the same originating contour on W. Moving on W away from a zero, when the curve $D = C$ is reached, one caustic is formed at infinity ($C_2 = 0$) while the other is at level $\frac{1}{2}\rho$. For contours with $D > C$ one caustic is virtual while the other is real, lying between W and level $\frac{1}{2}\rho$.

3. OBSERVATION AND INTERPRETATION

We may ask how the various caustic branches, emanating from the different elliptic umbilic foci at level F, meet and interact together. We cannot see their architecture directly, but have to infer it from the changing topology of the caustic curves seen on a series of plane sections. In three dimensions one has to picture a brilliant gothic palace: pointed arches of light, on a microscopic scale, with the tilted triangular columns of different sizes springing from a polished floor, which reflects their tracery of interactions, not in the usual way of a mirror, but in an inverse fashion to be described later. The following description is based on observations of the near field of small water drops made with the aid of a microscope, but the observations will be interpreted in the light of the knowledge, from Thom's theorem, that in the geometrical optics approximation the only singularities can be the fold, cusp, swallowtail and elliptic umbilic (the hyperbolic umbilic is ruled out, as shown in appendix B, but can be realized by adding the effect of gravity (see § 6)).

Starting with the microscope focused on the plane of the drop itself (with the whole drop bright so as to be sure that the angular aperture of the microscope is great enough to admit rays from all parts) and moving the plane of focus upwards (figure 4a to c and figure 5a to g) one sees a caustic-like line, containing many outward-pointing cusps, move inwards from the periphery of the drop. This is not at first a true caustic (because the curvature of W, and therefore of the drop, would in that case have to be infinite) but is a refracted shadow of the edge of the drop, complicated by the edge diffraction. (It is analogous to the Becke line used by mineralogists as a test of refractive index.) Such edge effects are not our primary concern.

As the plane of focus is continuously raised the caustic-like line becomes a true caustic, and it commonly contains several tens of cusps. In three dimensions the edge of the caustic is the locus of the lower of the two centres of curvature of the wavefront W at its periphery. It is like the edge of a ribbed skirt, or the edge of an umbrella; note that the ribs of the umbrella, the cusp lines, protrude upwards not downwards. As the plane of focus is raised, pairs of neighbouring cusps appear to merge together, which would be contrary to Thom's theorem; but closer examination shows that the sequence must be that of figure 6*a*, *b*, *c*. Without diffraction the process would be a beak-to-beak interaction which leaves a single cusp in the original caustic together with a small cusped triangle. However, the diffraction effect at the small triangle is usually so large that it is not seen as in figure 6*c* but rather as in figure 6*d*, a bright cusp being accompanied by a weak diffraction 'star'. Note the orientation of the star with respect to the triangle. The cusped triangle is a non-singular section of an elliptic umbilic, but its star-shaped diffraction pattern (Trinkaus & Drepper 1977; Berry, Nye & Wright (to be published)) is hard to distinguish from the pattern from a singular section; thus one has the erroneous impression that an elliptic umbilic singularity has already been formed. An example is seen in the lower right hand corner of figure 4*a* to *c*.

As the plane of focus moves higher still a complex sequence of interactions takes place among the caustic curves which may nevertheless be analysed into only two basic processes: (A) simple beak-to-beak, and (B) beak-to-beak and two swallowtails. Process (A) is essentially the same as figure 6, a separation of a caustic into two parts by pinching off at a beak-to-beak, but with the difference from figure 6 that both parts may have more than three cusps and they are large enough so that neither caustic is lost in diffraction. A number of examples occur between figures 5*c*, *d* and *e*. Process (B), shown in figure 7, is illustrated by Thom (1975, p. 86) as part of the universal unfolding of the parabolic umbilic. Focusing upwards one moves from figure 7*a* to *f* via swallowtails at S'_1 and S'_2 and a beak-to-beak joining (*d* to *e*). However, in the microscope, one commonly sees only the disappearance of the cusp in figure 7*a* to give the fold and diffraction star of figure 7*g*, the inferred intermediate detail of the caustic being submerged in diffraction (Berry & Nye 1977). It is notable that the diffraction star always orients itself as shown in figure 7*g* when it comes close to the fold. An example is the cusp indicated by the arrows in figure 5*c*, which has disappeared in figure 5*d* to leave a diffraction star almost entirely lost in the bright field of the fold. However, the diffraction star later becomes clearly visible as it emerges on the lower side in figure 5*e*. Several other examples can be traced in figure 5*c* to *g*.

The result of many elementary processes of the kinds just described is that at level F (figure 5*g*) there are no caustics left, the last one having become a cusped triangle and then collapsed to a bright elliptic umbilic diffraction star to join the other tens of similar diffraction stars already in the field. Thus the field at F consists entirely of diffraction stars; it is a remarkable sight. (Close inspection shows that the elliptic umbilic foci, while close to a single plane, are in fact at slightly different

heights; a difference of 2 mm in height was once observed. This could either be an effect of gravity, which causes the drop to have non-uniform pressure, or of the breakdown of the approximation of small slopes – more likely the former.)

Above level F similar processes are repeated. Locally, each process is like one of figures 6 or 7 read in reverse order, but the sequence in which the various beak-to-beak or piercing processes occur is quite different. Figure 11 shows a simple example of this where a 4-cusped caustic in the far field becomes two 3-cusped triangles, and then two elliptic umbilics at level F; below F the umbilics open out in the same orientation as before but then the two triangles interact in a different way by piercing through one another; a beak-to-beak and then two swallowtails finally produce at height $\frac{1}{2}\rho$ a 4-cusped caustic which is conjugate to the original one.

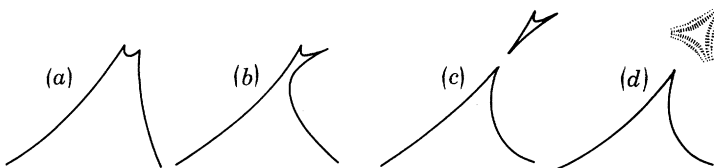


FIGURE 6. Two cusps of a caustic branch become one by pinching off a small cusped triangle, (a) to (c), but only the star-shaped diffraction pattern of the triangle is in fact seen (d).

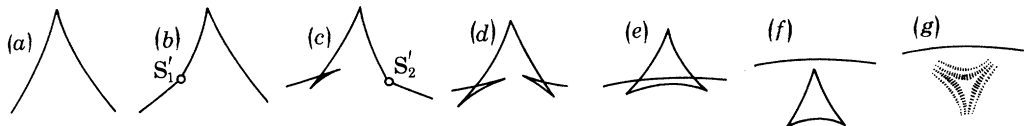


FIGURE 7. Process (B). Swallowtails S'_1 and S'_2 occur at (b) and (c) and a beak-to-beak occurs between (d) and (e). The final result (f) is that the cusp in (a) has been eliminated and a small cusped triangle has been formed. But the triangle is in fact only manifested by its diffraction pattern as seen in (g).

4. RELATION OF THE CAUSTICS TO THE WAVEFRONT

We now discuss how the features of the caustics arise from the topography of the drop itself, or, what is almost the same thing, from the topography of the wavefront W immediately above the drop. For points below F this is conveniently done in terms of the family of lines on W whose direction at any point is that of the greater principal curvature C_1 , together with the contours of the D -landscape. One is not free to specify both these families quite independently. The justification that they can lie as drawn in the figures that follow is given in § 5, where we analyse the caustics of a special symmetrical drop; the configurations drawn can be regarded as generic perturbations of this non-generic case.

At a given level the caustic is formed by rays that originate on a certain contour of C_1 , and therefore of D . Each separate branch of the caustic comes from a separate branch of the corresponding D contour. The cusps on the caustic arise from points where the contour is parallel to the direction of the curvature C_1 (the proof is

virtually the same as that given by Berry (1976) for the far field). Consider, for example, the neighbourhood of an elliptic umbilic point (figure 8). On a screen placed at a level just below F the caustic comes from the contour D_1 on W. Its three cusps P, Q, R come from the points p, q, r where the contour touches the curvature lines. At a slightly lower level the caustic comes from the neighbouring contour D_2 and its three cusps come from the points p', q', r' . The locus of p is called a *rib-line* on W and it gives rise to a cusp line or a *rib*, the locus of P, in the

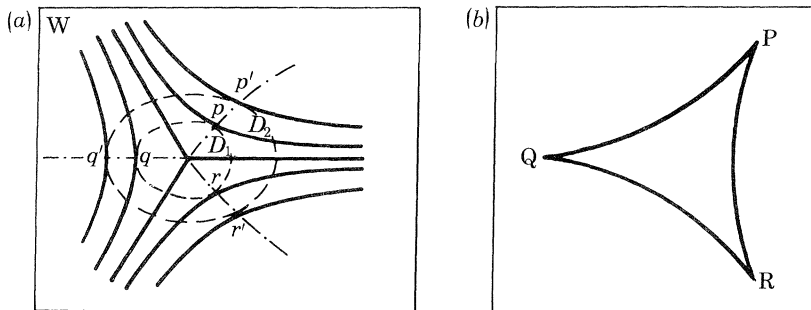


FIGURE 8. (a) The wavefront W near an elliptic umbilic point. —, direction lines of the curvature C_1 ; ---, contour lines of D ; -·-, rib-lines, where a contour of D is parallel to the direction of C_1 . (b) The caustic pattern at a height above the wavefront corresponding to the contour $D = D_1$.

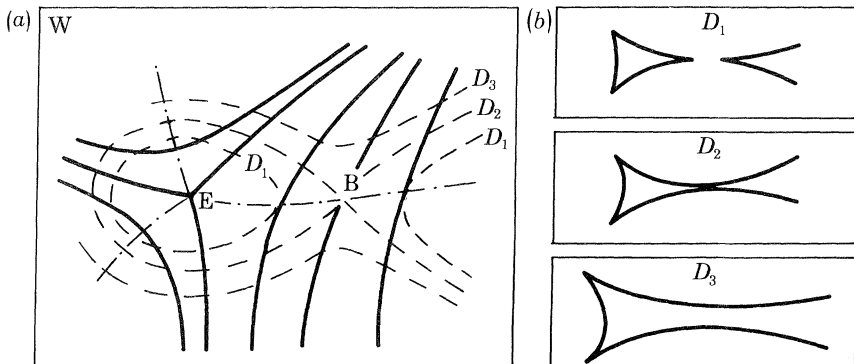


FIGURE 9. (a) One possible configuration for the wavefront W near a saddle point B for D . E is an elliptic umbilic point. —, direction lines of C_1 ; ---, contours of D ; -·-, rib-lines. (b) Caustic patterns at heights above the wavefront corresponding to contours $D = D_1, D_2$ and D_3 .

three-dimensional image space. At an elliptic umbilic point on W, three rib-lines come together and in the image space (figure 3) three ribs come together and touch. For levels above F we have to draw the directions of C_2 , orthogonal to those of C_1 , but the same D contours. Three rib-lines now leave the umbilic point and give rise to three ribs above the focus.

This is the local configuration near each zero in the D -landscape. Now consider

a saddle point B of the D -landscape (figure 9a). Here the D contour ($D = D_2$, say) crosses itself at right angles, as shown in appendix A. Suppose B to be near an umbilic point E and suppose we are below the level F. Since the only singularities of curvature direction are at umbilic points, the curvature C_1 at B has a definite direction. In figure 9a this direction is drawn to lie in the two sectors where $D > D_2$. By drawing the contours of D near $D = D_2$ we can see that a rib-line passes through B. At a screen height corresponding to D_1 ($D_1 < D_2$) there are two D_1 contours, two crossings of the rib-line and so two cusps (figure 9b). At a height corresponding to D_2 the two cusps both come from B, and therefore coincide, while at the height corresponding to D_3 ($D_3 > D_2$) there are no cusps. This configuration near B therefore gives a beak-to-beak event, which we have called process (A), on the moving screen.

But there is another possibility for the direction of C_1 at B, namely that it lies in the two sectors where $D < D_2$. We can show that this can result in process (B), beak-to-beak and two swallowtails, on the moving screen. Figure 10 shows two elliptic umbilic points, E_1, E_2 , with their associated curvature lines. Starting from the $D = 0$ point contour at each umbilic we imagine D increased continuously (this corresponds to lowering the screen from F) and, by following the intersections of the successive D contours with the rib-lines, we trace the evolution of the cusps on the screen (figure 11c to h). The contours at first cross the three rib-lines from each umbilic, forming two cusped triangles on the screen (figure 11d). When we reach the contour $D = D_2$ which crosses itself at B, two new rib-lines suddenly appear, marked 1 and 2; this is a beak-to-beak event on the screen (figure 11e and f), but, unlike figure 9, two cusps are created rather than destroyed. Note that a contour with $D > D_2$, such as the one marked with a dotted line, can make three intersections J, K, L with a given curvature line, and that as D increases a place S_1 is reached where the D contour is not only tangent to a curvature line but also crosses it. This produces the swallowtail S'_1 in the image space, where two cusps (2 and 7) merge and leave a smooth caustic. On W the rib-line is tangent both to the D contour and to the curvature direction. At a slightly higher D contour a similar configuration occurs on the other side at S_2 , giving the second swallowtail needed for process (B). Still higher contours of D encounter only the four rib-lines marked 3, 4, 5, 6, which correspond to cusps in the image space that have survived throughout the whole process.

The sequences just described account for the main features seen in the evolving caustics from an irregular droplet as one focuses downwards from the level F. Starting with many $D = 0$ points (elliptic umbilics) the contours of increasing D encounter a succession of saddle points. At some of them the curvature directions are like figure 9a and at others they are more like figure 10. Eventually, if the drop shape is not too complicated (for example, not having multiple summits), by the time the contour $D = C$ is reached we have climbed high enough up the bowl-shaped D landscape for the main branch of the contour to enclose nearly all the zeros. However, some deep and steep-sided zeros may still lie outside it. If it were not for diffraction, these would give a series of small cusped triangles detached

from the main caustic. But their extreme localization enhances diffraction and so they are seen merely as diffraction stars. Their appearance is misleading; it is as if we are looking at the diffraction pattern corresponding to the singular section of an elliptic umbilic; but we are not. Because of the great elongation of the diffraction

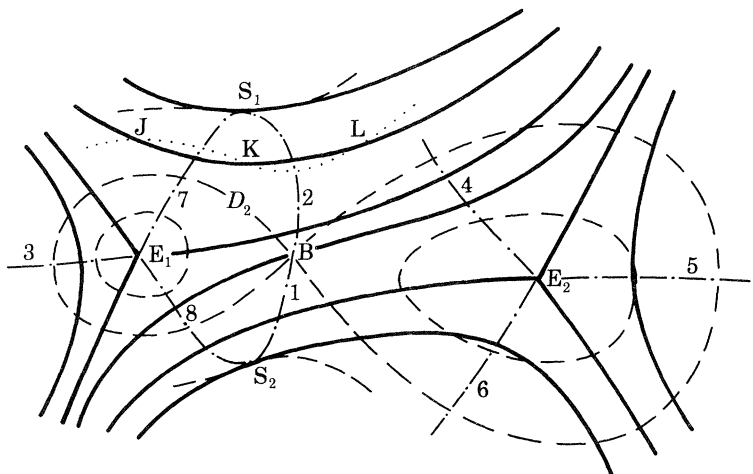


FIGURE 10. Alternative configuration of the wavefront W near a saddle point for D . The points S_1 and S_2 in the wavefront produce swallowtail catastrophes in the space above the wavefront.

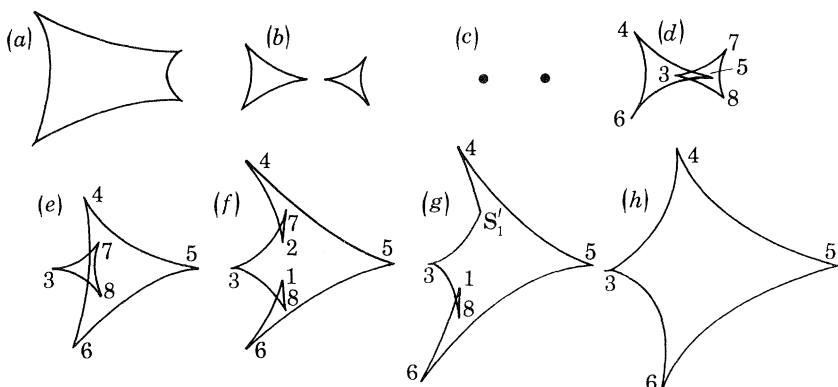


FIGURE 11. Caustic patterns produced by the wavefront of figure 10. (c) is the plane F and (a) to (h) are at levels successively closer to the drop. The numbering of the cusps corresponds to the numbering of the rib-lines in figure 10.

pattern in the axial direction its appearance is virtually the same at all levels. In fact, if we now focus upwards and follow one of these star patterns, we see it drift continuously across the whole field, persisting without interaction through level F and finally into the far field where it appears once again as a diffraction star outside the main caustic.

The focusing sequence above F, with its beak-to-beaks and swallowtails, is explained in the same way as the sequence below F, the only difference being that one has to draw the directions of the lesser curvature C_2 instead of those of C_1 . The D contour sequence is the same. A small element of a D contour produces a small length of caustic below F and another small length at the conjugate point above F, the two lengths being at right angles, in fact two focal lines. The two caustics at conjugate levels are always related in this way. So far as interactions in the caustics are concerned a given saddle point in D will give a beak-to-beak not only below F but also at the conjugate point above F, the two being arranged at right angles as focal lines. The direction lines of C_2 are orthogonal to those of C_1 , and so figures 9a and 10 become, in a general way, interchanged; process (A) below F tends to be associated with process (B) above F. It is in this sense that the interactions of the caustics above F are inverse to their interactions below F.

The relation between the caustics at two conjugate levels is seen very clearly if we look at the pattern of cusps from near the edge of a drop. In figure 12b the microscope is focused on the drop itself, in figure 12a it is focused just above and in figure 12c just below, so that the caustic is virtual. The cusps above the drop can be seen to alternate with those below, a cusp above being associated with an uncusped piece of caustic below and vice versa. In fact the cusps above the drop come from salients in the boundary while those below come from re-entrants. (The virtual caustic below the drop is not well seen in the ordinary way because it appears outside the edge of the drop and is swamped by the direct light. Figures 12a, b, and c were made by sticking a piece of opaque tape to a glass slide, cutting a roughly square hole in the tape and then placing a water drop in the hole; the direct beam is thus masked out. The figure shows only part of the hole.) The fact that the number of cusps on the main caustic figure is greater near the edge of the drop presumably means that the D landscape is more irregular there. In a drop resting on a bare piece of glass this is a consequence of the rapid spatial variations of the contact angle around the edge; in a drop formed by the hole-in-tape method it results from imperfections in the edge of the tape. In both cases, because the governing differential equation is elliptic, the effects of fluctuations in the boundary condition are damped out quite rapidly.

In the whole focusing sequence one only rarely sees the lips event. This would result from a local maximum in the D landscape and, as we have noted, the surface tension equation precludes maxima. Those lips events that have been seen with drops on a horizontal surface were with small, nearly spherical, drops where the neglect of gravity, which causes a pressure gradient in the drop, is suspect.

5. A NON-GENERIC SPECIAL CASE

Our main discussion has been about generic caustics in three-dimensional space: there has been no special symmetry. It still remains to make sure that the general relations between D contours and curvature lines shown in figures 9a and 10 can

be realized. For this purpose we now consider explicitly a symmetrical drop with two umbilic points, for figures 9*a* and 10 can then be regarded as perturbations of this symmetrical case: the generic catastrophes in three-dimensional control space are an unfolding of the non-generic case to be calculated.

Following Berry (1976) we note that the general solution of equation (4) is

$$f(x, y) = \frac{1}{4}C(x^2 + y^2) + \operatorname{Re} g(x + iy), \quad (8)$$

where $g(x + iy)$ is any analytic function. In general, the expression for the curvature difference, D , is

$$D = +\{(f_{xx} - f_{yy})^2 + 4f_{xy}^2\}^{\frac{1}{2}}, \quad (9)$$

where suffixes denote differentiation. Writing

$$g(\zeta) = u(x, y) + iv(x, y), \quad (\zeta = x + iy), \quad (10)$$

where u and v are real functions, and using equation (8) we have

$$D = +2(u_{xx}^2 + u_{xy}^2)^{\frac{1}{2}} = 2|g''(\zeta)|. \quad (11)$$

Thus the contours of D are those of $2|g''(\zeta)|$.

We examine the drop generated by

$$g''(\zeta) = K(1 - \zeta^2/l_0^2), \quad (12)$$

where l_0 is a length and K is a real positive constant with dimensions [length] $^{-1}$. This is the drop whose far-field caustic as the pressure p varies was discussed by Berry. In this analysis, on the other hand, we keep p , and therefore C , constant and we are concerned with the variation of D over the wavefront. There are two points of zero D at $(\pm l_0, 0)$. These are umbilic points, not to be confused with summits of the drop, of which there is only one, at the origin. Taking l_0 as the unit of length, integrating equation (12) and substituting in equation (8) shows that the equation for the wavefront W in polar coordinates (r, θ) is

$$f = \frac{1}{4}r^2(2K \cos 2\theta + C) - \frac{1}{12}Kr^4 \cos 4\theta. \quad (13)$$

We have omitted the term in r and the constant as representing merely an inessential tilt and change of zero. Figure 13 sketches the lines of constant D and the direction lines for C_1 . We wish to examine the contact between the two families of lines on $x = 0$. The D contour intersecting $x = 0$ at the general point $y = y_0$ has the form

$$y = y_0 + \frac{1 - y_0^2}{2y_0(1 + y_0^2)}x^2 + \dots \quad (14)$$

On the other hand, the direction of C_1 is given by

$$\tan 2\psi = \frac{f_{xy}}{f_{xx} - \frac{1}{2}C},$$

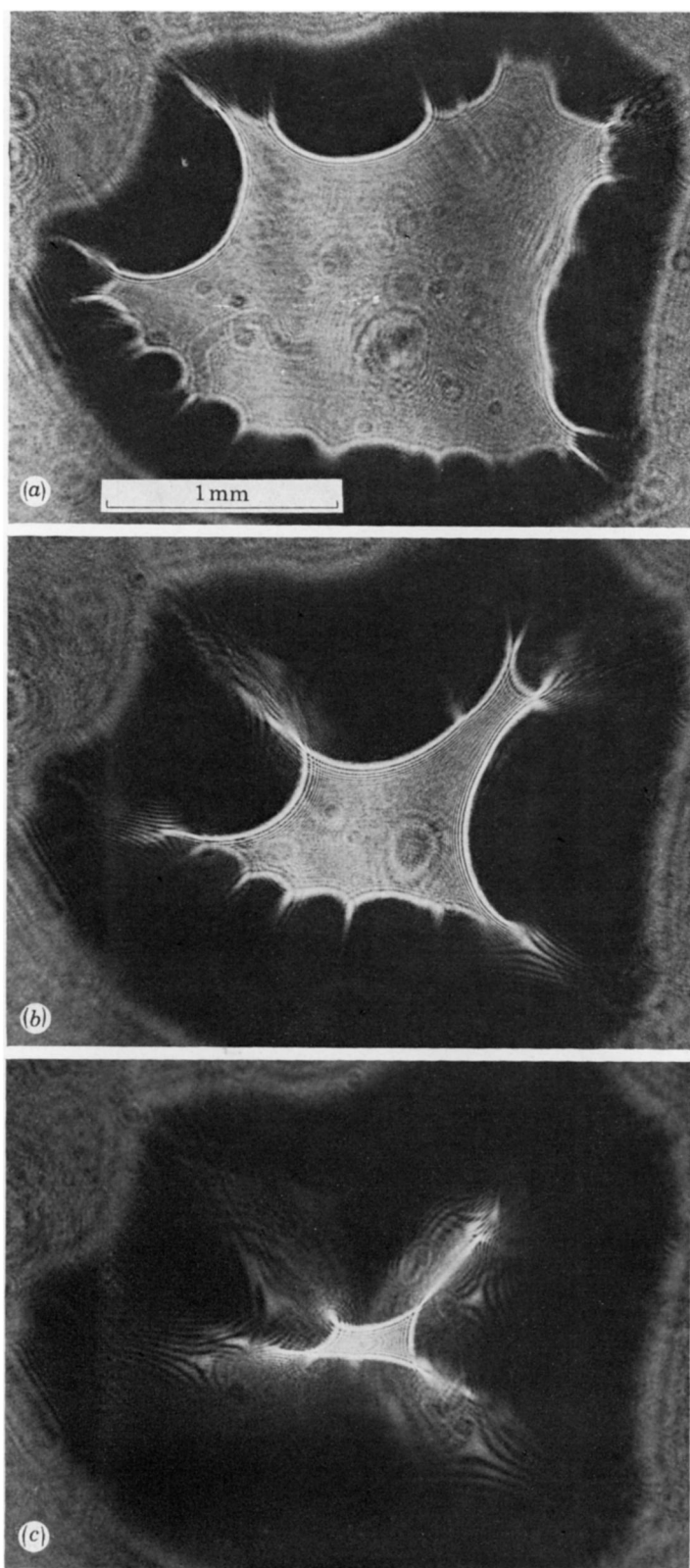


FIGURE 4. (a)–(c) A small drop on a glass slide is illuminated with parallel light from a laser (wavelength 633 nm). Photographs of the caustic structure as the plane of focus of the microscope moves away from the drop.

(*Facing p. 32*)

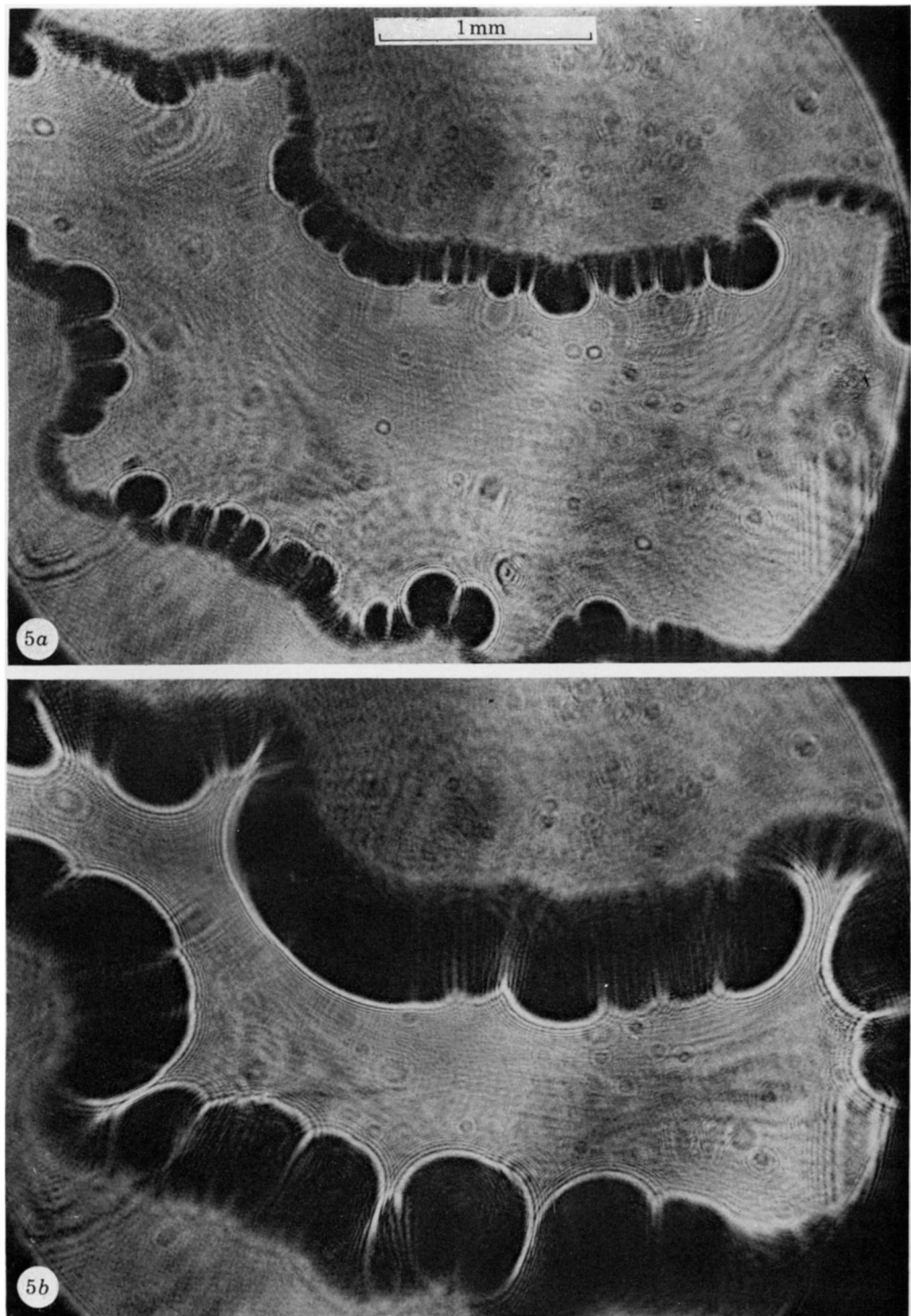


FIGURE 5. (a)–(g) As figure 4 but a different drop. In (a) the microscope is focused just above the drop and in (g) it is focused on the plane F where all the elliptic umbilic foci lie.

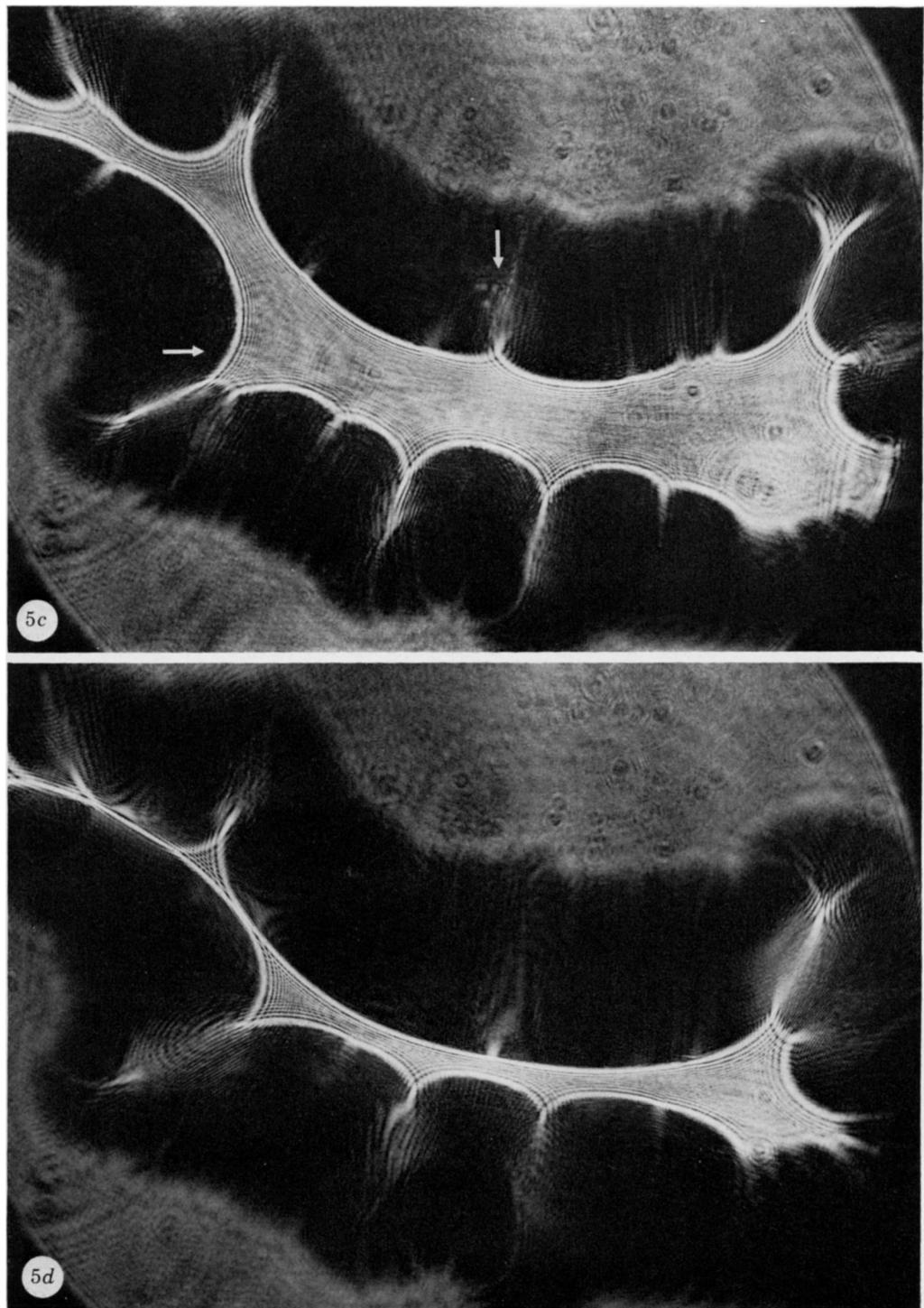


FIGURE 5 *c, d.* For legend see plate 2.

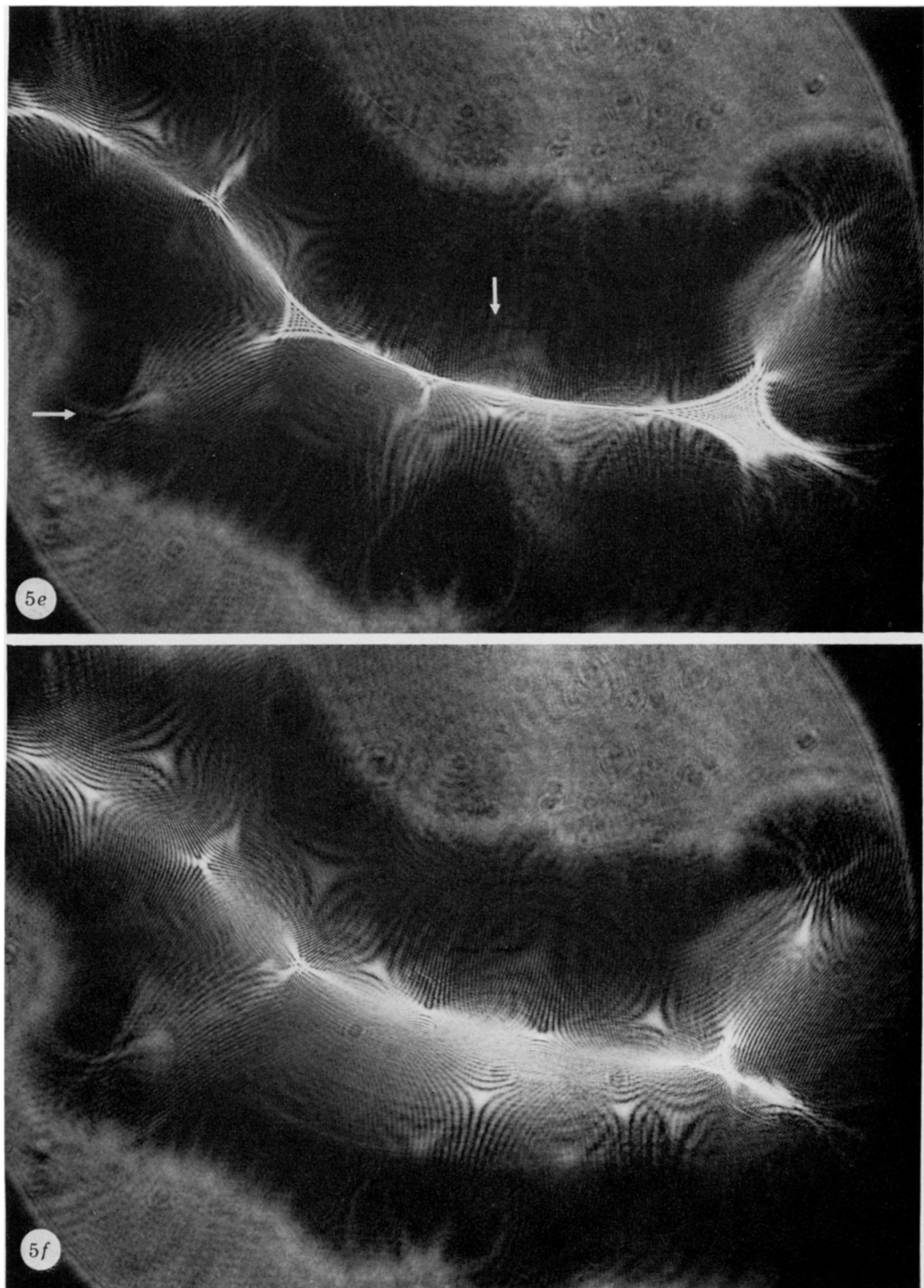


FIGURE 5 *e, f*. For legend see plate 2.

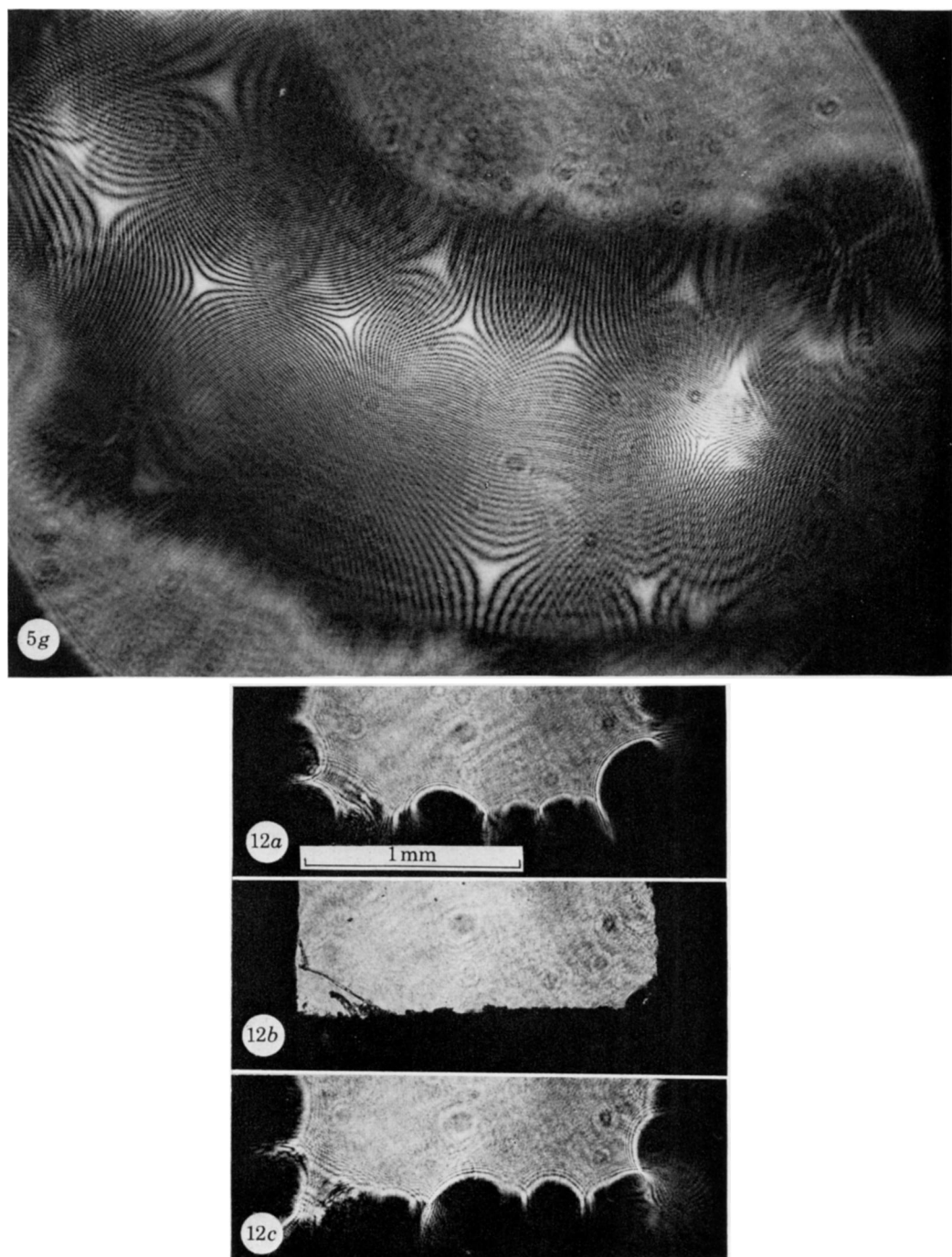


FIGURE 12. The plane of focus is (a) above, (b) at, and (c) below the plane of a drop. The cusps alternate, so that the caustics at the two approximately conjugate levels are at right angles to each other, like focal lines. A very clear example appears in the bottom right hand corner.

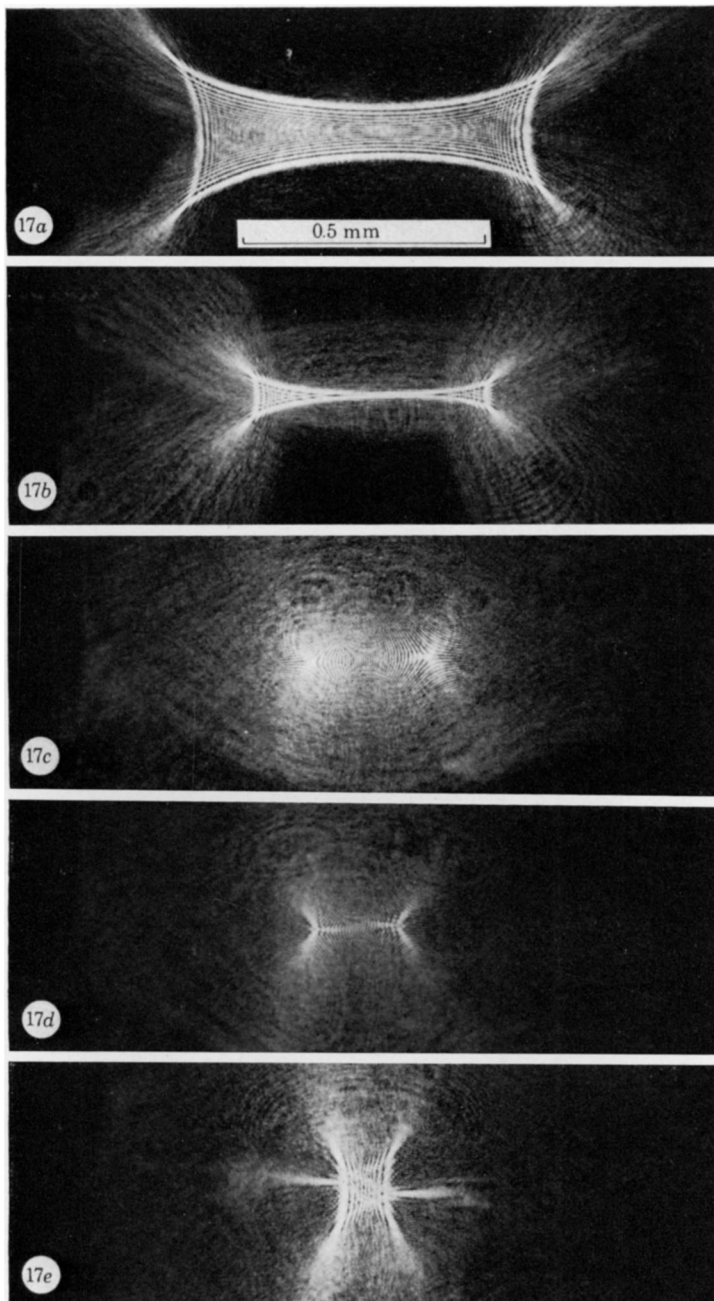


FIGURE 17. A drop rests on a glass slide and its edges are defined by a roughly rectangular hole cut in a piece of tape stuck to the glass. Photographs of the caustics seen as the plane of focus of the microscope is successively moved away from the drop. (a) Like figure 16c, (b) like figure 16b, (c) the plane F; like figure 14a, (d) like figure 14b, (e) like figure 14d (f) like figure 14e, (g) like figure 14f, (h) like figure 14g.

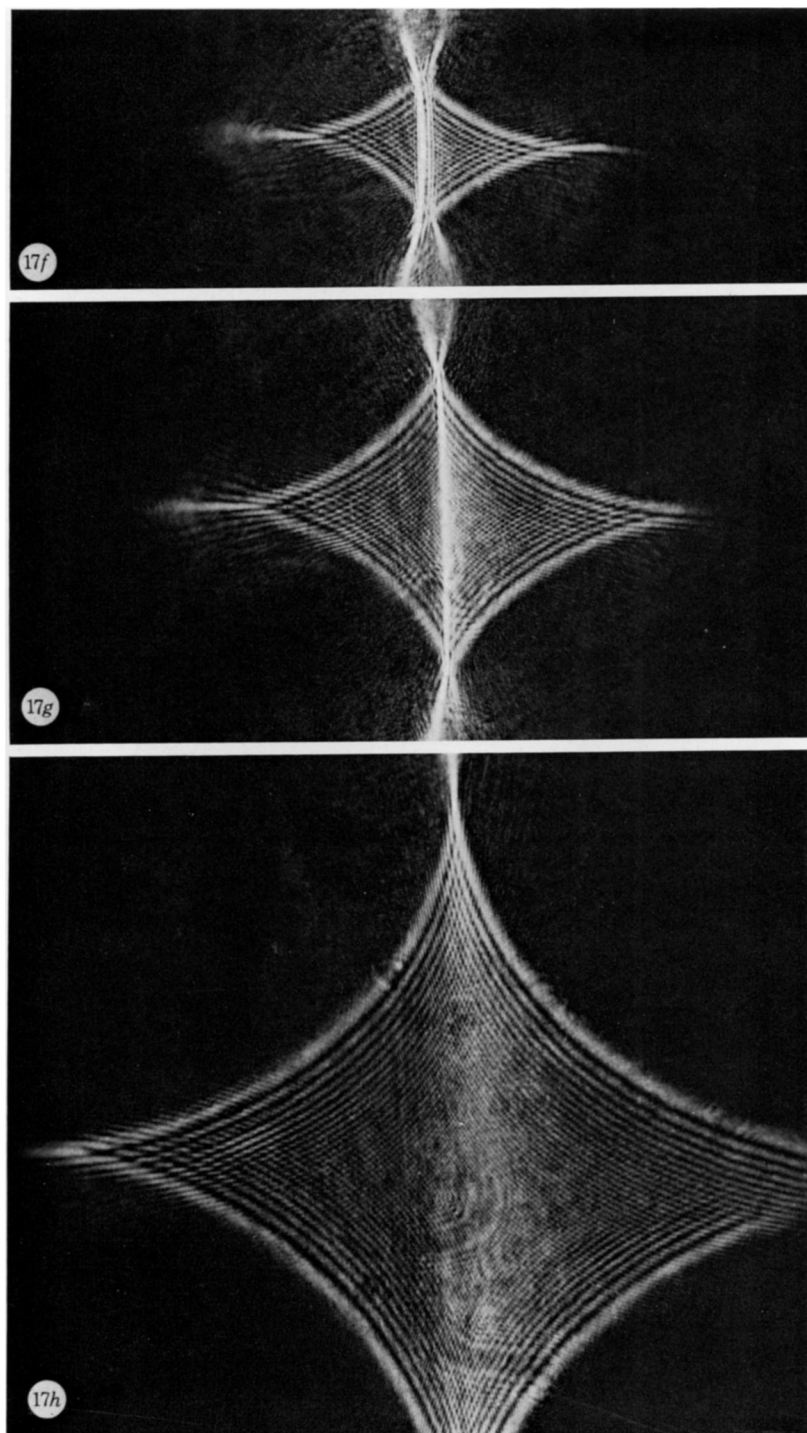


FIGURE 17*f-h*. For legend see opposite.

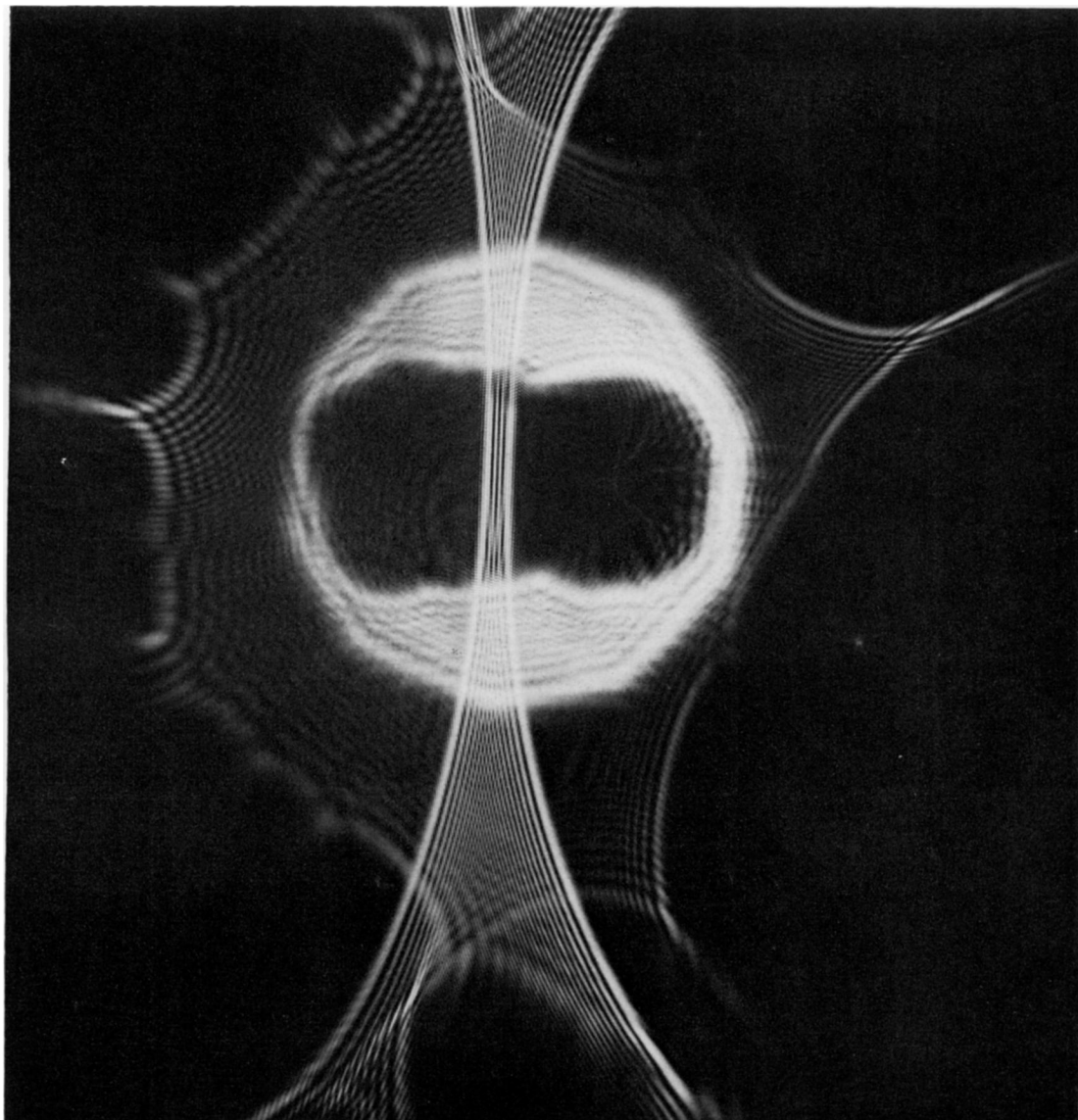


FIGURE 18. The far-field caustic of a drop with a double summit. This photograph, unlike all the others, was not taken with a microscope; a broadened laser beam was incident on the drop and the film placed to record the far field, without any lenses. The shadow of the drop against the direct beam is seen in the centre.

where $\tan \psi$ is the slope dy/dx . Expansion about $(0, y_0)$ and integration then gives for the equation of the direction line

$$y = y_0 + \frac{y_0}{2(1+y_0^2)} x^2 + \dots \quad (15)$$

The D contour and the direction line are identical to order x^2 when $y_0 = \pm 1/\sqrt{2}$. These are the points B_1, B_2 (figure 13) where a line from one family makes higher-order contact with a line from the other family.

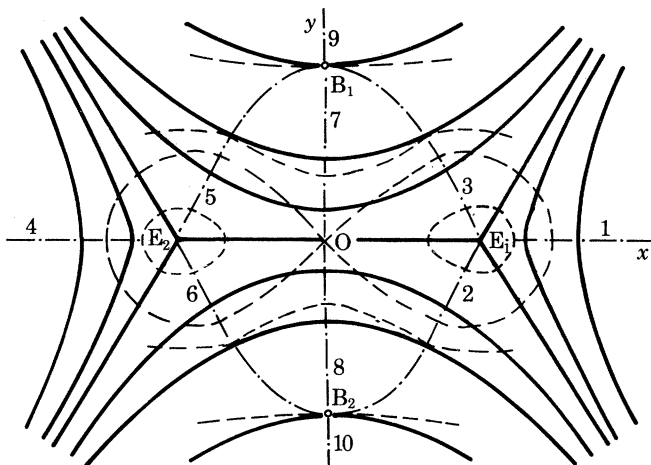


FIGURE 13. The wavefront of equation (12) with K real and positive. E_1 and E_2 are elliptic umbilic points. —, direction lines of C_1 ; ---, contours of D ; -·-, rib-lines. Points B_1 and B_2 give butterfly catastrophes in the caustics above the wavefront.

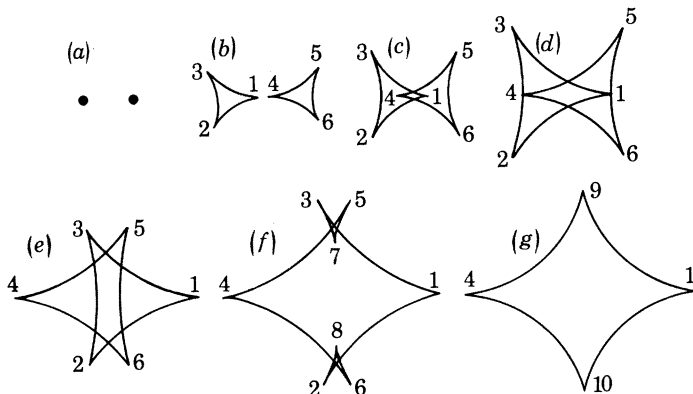


FIGURE 14 (a)–(g). Sequence of caustics produced by the wavefront of figure 13, starting at the plane F containing the two elliptic umbilic foci and moving successively closer to the drop. Between (b) and (e) the two caustics pass through one another without interacting. There is a beak-to-beak between (e) and (f) and there are two simultaneous butterflies between (f) and (g).

The rib-lines take the forms sketched in figure 13. At O the higher curvature C_1 is along Ox and so the curvature in the x -direction at O is higher than it is at E_1 and E_2 . This causes the normals from E_1 and E_2 to cross below the plane of focus, F, and so the elliptic umbilic focus from E_1 lies to the left of that from E_2 (figure 14a, b). As we focus downwards from F, and D increases from zero, there are at first two triangles with cusps from the rib-lines 1, 2, 3 and 4, 5, 6. Double piercing takes place (figure 14d), with no interactions between caustics because whenever folds cross they come from different contour loops, until the critical contour through O is reached. Then two new cusps, 7 and 8, are born (beak-to-beak) and a D contour now encounters eight rib-lines, giving eight cusps. This continues until the next critical contour, through B_1 and B_2 , is reached. There are two simultaneous butterfly catastrophes (appendix C): two sets of three cusps merge to leave cusps 9 and 10, and below this level we are left with these two cusps plus cusps 1 and 4 which remained present throughout. (The fact that the two butterflies are simultaneous is trivial, in that they merely have the same Z coordinate.)

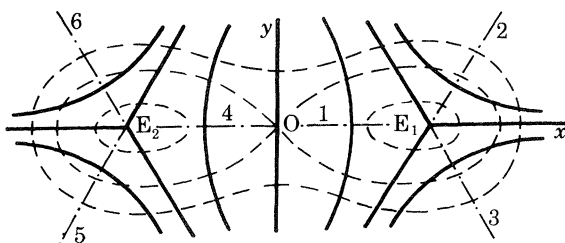


FIGURE 15. As figure 13 but with the full lines showing the direction of C_2 .

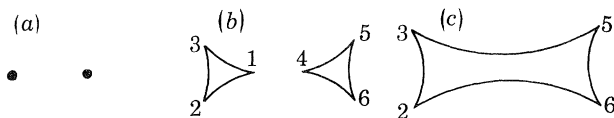


FIGURE 16. (a)–(c) Sequence of caustics produced by the wavefront of figure 15 starting at plane F and moving away from the drop.

Returning to the plane F and focusing upwards, the D contours are the same but we are now dealing with the lines of C_2 . Figure 15 shows the configuration on the wavefront and figure 16 shows the caustics. Starting at $D = 0$, two three-cusped triangles open out until at the critical D contour through O, cusps 1 and 4 annihilate at a beak-to-beak, conjugate to the beak-to-beak that occurred below F. Above this the four cusps 2, 3, 5, 6 continue into the far field; there is no special event conjugate to the two butterflies below F.

If we take K in equation (12) as real and negative, the wavefront (13) gives the two butterflies above F rather than below. Figure 14, or part of it, is now the sequence above F while figure 16 is the sequence below. A good approximation to this case is seen in figure 17a to h, with the fine details of the transitions masked

by characteristic diffraction patterns. Figure 17*c* shows the plane F; thus figure 17*c* to *h* correspond to figure 14*a* to *g*. For this series of pictures a roughly rectangular hole was cut in a piece of tape stuck to a glass slide, and the drop was made to span the hole.

Continuing the case of K real and negative, we find that, on $x = 0$,

$$C_2 = \frac{1}{2}C + K(1 + y^2),$$

and at $y^2 = \frac{1}{2}$, corresponding to B_1 and B_2 in figure 13,

$$C_2 = \frac{1}{2}(C + 3K).$$

Thus if $C = -3K$ the butterflies are produced in the far field. We can regard this condition as defining a critical value of K , for fixed C , or a critical C for fixed K . The latter interpretation gives a critical pressure in the drop of $-3K\gamma/(n-1)$. As the pressure passes through this value the number of cusps in the far field will change from four to eight without any alteration in the number (two) of zeros of g'' within the contour $D = C$. This contradicts Berry's general result (1976, p. 13) that there are two more cusps in the far field than $g''(\zeta)$ has zeros within the contour $D = C$. In fact this general result always seems to be violated when there are swallowtails or butterflies 'beyond' the far field. For K sufficiently negative ($K < -\frac{1}{2}C$), but not otherwise, the drop has two summits. Figure 18 shows an example of the far field of an irregular drop having two summits. The two close caustics passing near the centre of the field are conspicuous features of such drops and they correspond to the two that appear in figure 14*e*.

As a more general case let us now take K in equation (12) as complex. If we discard terms of higher order than r^2 , (12) and (8) give for the wavefront W sufficiently near to O

$$f(r, \theta) = \frac{1}{4}Cr^2 + \frac{1}{2}|K|r^2 \cos(2\theta + \alpha),$$

where $K = |K|e^{i\alpha}$. Thus the term containing C contributes a spherical curvature and, by itself, would give an indeterminate direction at O for the lines of curvature. Their direction is decided by the term containing $|K|$, which represents the addition of a saddle in W at O. The orientation of the saddle is fixed by the argument α of K . On the other hand, the D contours, being given near O by

$$D = 2|g''(\zeta)| = 2|K|,$$

from (11) and (12), are unaffected by the argument of K . We have already considered the cases $\alpha = 0$ and π . When $\alpha = \frac{1}{2}\pi$ (figure 19*b*) the saddle is oriented so that the directions of curvature at O make an angle $\frac{1}{4}\pi$ with Ox and Oy. Thus in this case the direction of C_1 , say, is parallel to the D contour at O. This is the transitional case between the processes we have called (A) and (B). It means that in the space above the wavefront we expect something intermediate between a simple beak-to-beak and a beak-to-beak accompanied by two swallowtails. Figure 19*a, b, c* sketches the wavefront and the caustic at the level of the beak-to-beak

as α passes through $\frac{1}{2}\pi$. As α reaches $\frac{1}{2}\pi$ the two swallowtails meet and annihilate (just as, in one lower dimension, two cusps can meet and annihilate at a beak-to-beak).

For these drops generated by equation (12), since $g(\zeta) = g(-\zeta)$, $f(x, y)$ is always centrosymmetrical about O. Thus the two umbilic foci, their diffraction patterns and their unfoldings, are always related centrosymmetrically. As the argument α of K changes, the D contours remain the same while the direction lines of C_1 around each umbilic rotate, the sense of rotation being the same for both umbilics. In

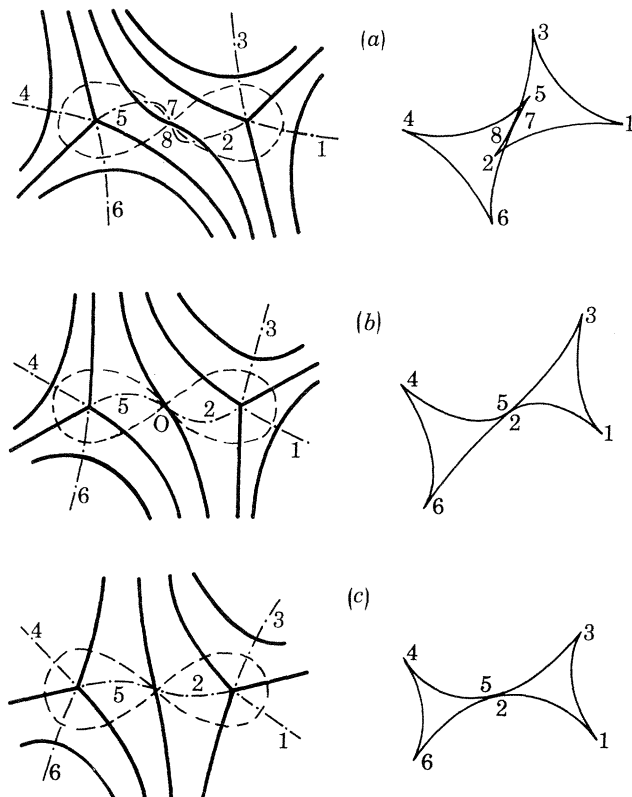


FIGURE 19. The interaction of two cusped triangles. In (a) a beak-to-beak is accompanied by two swallowtails; in (b) the two swallowtails merge ($\alpha = \frac{1}{2}\pi$); in (c) there is only a beak-to-beak. On the left is the wavefront and on the right the caustic. Notation as in figure 13.

general droplets there are many umbilic foci, but it is noticeable that when there are two which are not only close but also interact (showing that they come from close points on the drop) their diffraction stars are always related centrosymmetrically.

Drops with only two umbilics in the central region can be made quite easily by the hole-in-tape method. A rhombus-shaped hole is observed to give the case K

real and positive, while a rectangular hole, as we have seen, gives the case K real and negative. Other parallelograms give intermediate cases with K complex. Of course this correspondence is only for the central region because the drops generated by equation (12) do not have straight edges.

6. DROPS UNDER GRAVITY

In conclusion, we remark that if the water droplet is on a vertical surface the effect of gravity becomes significant even for drops 1 mm or so in size. In fact, by tilting a given drop the relative size of the gravitational effect can become an additional control parameter.

In a horizontal drop with small slopes an elliptic umbilic focus cannot lie on a fold, because all elliptic umbilic foci are at level F and there can be, generically, no folds at this level (they would need lines rather than points of zero D). But by varying an additional control parameter, such as angle to the vertical, to give four control parameters in all, one can make an elliptic umbilic catastrophe have its singularity precisely on a fold, and then one has the parabolic umbilic. By changing the parameter still further and thus unfolding the parabolic umbilic in a different way, one obtains the hyperbolic umbilic. Hyperbolic umbilic foci are readily observed in vertical droplets. (One is often seen partly unfolded, at the top of the far field looking through a droplet at a point source with the unaided eye.) By suitable variation of the four control parameters it is in fact possible to produce the whole sequence of unfolding of the parabolic umbilic (as, for example, on p. 86 of Thom (1975)).

Rotation of a tilted drop in its plane, its periphery being fixed on the rotating glass substrate, provides a further control parameter, with the possibility of producing catastrophes of codimension 5. These matters will be pursued in another paper.

It is a pleasure to acknowledge the invaluable advice of Dr M. V. Berry, particularly on the use and applicability of Thom's theorem and in the analysis of appendix C. I should also like to thank Mr C. Upstill for commenting on a draft of the paper.

APPENDIX A. FEATURES OF THE D -LANDSCAPE

We first show that the sum of the principal curvatures of the D -landscape is never negative.

In terms of the derivatives of $f(x, y)$, to be denoted by suffixes, the sum C and the difference D of the principal curvatures are given by

$$C = f_{xx} + f_{yy} \quad (\text{A } 1)$$

$$\text{and} \quad D = +\{(f_{xx} - f_{yy})^2 + 4f_{xy}^2\}^{\frac{1}{2}}. \quad (\text{A } 2)$$

$$\text{Hence} \quad D = +\{(2f_{xx} - C)^2 + 4f_{xy}^2\}^{\frac{1}{2}} = +\{(2f_{yy} - C)^2 + 4f_{xy}^2\}^{\frac{1}{2}}. \quad (\text{A } 3)$$

Differentiation of (A 1) gives the relations

$$\begin{aligned} f_{xxxx} + f_{xxyy} &= 0, \\ f_{xxyy} + f_{yyyy} &= 0, \end{aligned}$$

from which

$$f_{xxxx} = f_{yyyy}.$$

Differentiating (A 3) and using these and similar relations yields for the sum of the principal curvatures of $D(x, y)$,

$$\begin{aligned} D_{xx} + D_{yy} &= -2\left(\frac{1}{2}D\right)^{-3}\{(Mu+Nv)^2 + (Mv-Nu)^2\} + 4\left(\frac{1}{2}D^{-1}\right)(u^2+v^2) \\ &= -2\left(\frac{1}{2}D\right)^{-3}(M^2+N^2)(u^2+v^2) + 4\left(\frac{1}{2}D\right)^{-1}(u^2+v^2), \end{aligned}$$

where

$$M = f_{xx} - \frac{1}{2}C, \quad N = f_{xy}, \quad u = f_{xxx}, \quad v = f_{xxy}.$$

Noting that

$$D^2 = 4(M^2 + N^2)$$

we find

$$D_{xx} + D_{yy} = 2\left(\frac{1}{2}D\right)^{-1}(u^2+v^2).$$

Since $D \geq 0$ the result is proved. We also see that when $D = 0$, at the umbilic points, $(D_{xx} + D_{yy})$ is infinite.

The D -landscape has degenerate conical minima at the zero level, but with these exceptions it has no maxima or minima; all the stationary points are saddles. We can see this as follows.

Since D is essentially positive it suffices to prove the property for D^2 . It follows from equation (11) that

$$D^2 = 4|g''(\zeta)|^2,$$

where $g(\zeta) = g(x+iy)$ is any analytic function. Near a stationary point of D^2 , $g''(\zeta)$ must be of the form

$$g''(\zeta) = A + B\zeta^2 + \dots,$$

where A and B are complex constants, with no linear term. Hence

$$|g''(\zeta)|^2 = AA^* + (AB^* + A^*B)(x^2 - y^2) - 2i(AB^* - A^*B)xy + \dots$$

Because the coefficients of x^2 and y^2 are opposite in sign the stationary point is a saddle. Moreover, because the coefficients are equal and opposite the contours of D^2 at the saddle cross at right angles. It follows that the contours of the D -landscape do likewise.

APPENDIX B. THE ELLIPTIC UMBILIC FOCI

We wish to examine the nature of the focus from a point on the wavefront $f(r)$ that is locally spherical. Consider the solution of equation (4) in polar coordinates (r, θ) in ascending powers of r up to r^3 :

$$f(r, \theta) = \frac{1}{4}Cr^2 + \alpha r^2 \cos 2\theta + \beta r^2 \sin 2\theta + ar^3 \cos 3\theta + br^3 \sin 3\theta.$$

The term $\frac{1}{4}Cr^2$ is a particular integral. In the complementary function, with arbitrary constants α, β, a, b , we have omitted the constant and linear terms by choosing the origin O on the wavefront and by taking the plane $z = 0$ tangential to the wavefront at O. If the wavefront is to be locally spherical at O, we must

take $\alpha = \beta = 0$, and by choice of the direction $\theta = 0$ we can take $b = 0$. Thus the wavefront is

$$f(r, \theta) = \frac{1}{4}Cr^2 + ar^3 \cos 3\theta,$$

or, in cartesians, $f(x, y) = \frac{1}{4}C(x^2 + y^2) + a(x^3 - 3xy^2)$.

With this wavefront we now expand the generating function (1) about the focus $(0, 0, 2C^{-1})$, using the new height variable

$$Z_1 = Z - 2C^{-1}.$$

Dropping terms of quadratic and higher order in the control variables (X, Y, Z_1) we obtain

$$\phi = a(x^3 - 3xy^2) + \frac{1}{8}C^2Z_1(x^2 + y^2) + \frac{1}{2}CXx + \frac{1}{2}CYy,$$

which apart from scale factors is a standard form for the elliptic umbilic catastrophe and its universal unfolding (Thom 1975, p. 75).

APPENDIX C. ANALYSIS OF A BUTTERFLY CATASTROPHE

In this appendix we examine the form of $f(x, y)$ near B_1 in figure 13 and show that the corresponding generating function has the form required for the butterfly catastrophe.

The wavefront (13) in Cartesian coordinates is

$$f(x, y) = \frac{1}{4}(C + 2K)x^2 + \frac{1}{4}(C - 2K)y^2 - \frac{1}{12}K(x^4 - 6x^2y^2 + y^4). \quad (\text{C } 1)$$

We move the origin to the butterfly point $(0, 1/\sqrt{2})$ and drop the constant and the linear terms, since they have no effect on curvatures, to give

$$f(x, y) = \frac{1}{4}(C + 3K)x^2 + \frac{1}{4}(C - 3K)y^2 + K\left(\frac{1}{\sqrt{2}}x^2y - \frac{1}{3\sqrt{2}}y^3 - \frac{1}{12}x^4 + \frac{1}{2}x^2y^2 - \frac{1}{12}y^4\right). \quad (\text{C } 2)$$

In the new coordinate system the wavefront is horizontal at the new origin. With the Z axis vertical, and thus normal to the wavefront, the lower of the two centres of curvature, where the butterfly exists, is at height $Z = 2/(C + 3K) = C_1^{-1}$. Thus henceforth the constant C_1 will denote the value of $C_1(\mathbf{r})$ at B_1 . We use the new height variable

$$Z_1 = Z - C_1^{-1}, \quad (\text{C } 3)$$

insert $f(x, y)$ in equation (1) for ϕ , and drop terms quadratic or higher in the control variables (X, Y, Z) to give

$$\begin{aligned} \phi = K &\left(-\frac{3}{2}y^2 + \frac{1}{\sqrt{2}}x^2y - \frac{1}{3\sqrt{2}}y^3 - \frac{1}{12}x^4 + \frac{1}{2}x^2y^2 - \frac{1}{12}y^4 \right) \\ &+ C_1(Xx + Yy) + \frac{1}{2}C_1^2Z_1(x^2 + y^2). \end{aligned} \quad (\text{C } 4)$$

To reduce this to a standard form first transform y to a new state variable y_2 :

$$y_2 = y - \frac{1}{3\sqrt{2}}x^2 + \lambda x^4, \quad (\text{C } 5)$$

where λ is a constant. (The coefficient of x^2 has been chosen to make the parabolic D contour and the direction line through B_1 reduce to $y_2 = 0$.) Keeping the lowest powers of x and y_2 only, this reduces the germ (the term in (C 4) not involving the control variables) to

$$K \left\{ -\frac{3}{2}y_2^2 + y_2 x^4 \left(3\lambda + \frac{5}{18\sqrt{2}} \right) + \frac{1}{8}x^6 \right\}.$$

So, choosing λ to make the coefficient of $y_2 x^4$ vanish, the germ has, apart from trivial scaling factors, the form $x^6 - y_2^2$ required for the butterfly (Poston & Stewart 1976, p 74).

Turning now to the part of (C 4) which involves the control variables, so as to examine the unfolding, we substitute for y using (C 5) and obtain

$$\phi = K(\frac{2}{8}x^6 - \frac{3}{2}y_2^2) + C_1 Xx + C_1 Y \left(y_2 + \frac{1}{3\sqrt{2}}x^2 \right) + C_1^2 Z_1 \left(\frac{1}{2}x^2 + \frac{1}{3\sqrt{2}}y_2 x^2 + \frac{1}{36}x^4 \right),$$

neglecting terms of higher order than Yx^2 and $Z_1 x^4$, and also neglecting the term in $Z_1 y_2^2$ in comparison with y_2^2 . To get rid of the term in Yy_2 replace y_2 by the new state variable y_3 ,

$$y_3 = y_2 - \frac{1}{3}K^{-1}C_1 Y \quad (\text{C } 6)$$

and drop terms quadratic in the control variables, to give

$$\phi = K(\frac{2}{8}x^6 - \frac{3}{2}y_3^2) + C_1 Xx + \frac{1}{3\sqrt{2}}C_1 Yx^2 + \frac{1}{2}C_1^2 Z_1 x^2 + \frac{1}{3\sqrt{2}}C_1^2 Z_1 x^2 y_3 + \frac{1}{36}C_1^2 Z_1 x^4.$$

The coefficient of x^2 suggests the new control variable

$$Y_1 = \frac{1}{3\sqrt{2}}C_1 Y + \frac{1}{2}C_1^2 Z_1 \quad (\text{C } 7)$$

and the term in $x^2 y_3$ can be absorbed into the one in y_3^2 by completing the square. Thus put

$$y_4 = y_3 - \frac{1}{9\sqrt{2}}K^{-1}C_1^2 Z_1 x^2, \quad (\text{C } 8)$$

and again neglect terms quadratic in the control variables, to give

$$\phi = K(\frac{2}{8}x^6 - \frac{3}{2}y_4^2) + C_1 Xx + Y_1 x^2 + \frac{1}{36}C_1^2 Z_1 x^4. \quad (\text{C } 9)$$

The butterfly catastrophe has four control variables while so far we have only three: X , Y_1 , Z_1 . The missing control is the one that makes the butterfly unfold unsymmetrically with respect to the x direction. To introduce this we must perturb the shape of the drop in a way that makes it no longer symmetrical about Oy . Such an unsymmetrical drop would give the caustics generic in three dimensions that are the primary concern of the paper. Since we are only interested at present in the local structure around B_1 a simple way is to add to $f(x, y)$ the extra part

$$e(x^3 - 3xy^2), \quad (\text{C } 10)$$

this being allowable because the new part satisfies Laplace's equation. ϵ is the new control variable. In terms of x and y_2 the new part is

$$\epsilon(x^3 - 3xy_2^2), \quad (\text{C } 11)$$

ignoring terms of higher order than ϵx^3 . The term in ϵxy_2^2 is small compared with y_2^2 in the germ. Thus we finally obtain for ϕ

$$\phi = K(\frac{2}{8}x^6 - \frac{3}{2}y_4^2) + C_1 Xx + Y_1 x^2 + \epsilon x^3 + \frac{1}{3}C_1^2 Z_1 x^4, \quad (\text{C } 12)$$

which, apart from scaling factors, is the standard form given by Poston & Stewart (1976, p. 74), the state variables being x and the 'inessential' y_4 , and the control variables being X , Y_1 , ϵ , Z_1 . The relations to the original variables, referred to B_1 as origin, are

$$\left. \begin{aligned} y_4 &= y - \frac{1}{3\sqrt{2}}x^2 - \frac{5}{54\sqrt{2}}x^4 - \frac{1}{3}K^{-1}C_1 Y - \frac{1}{9\sqrt{2}}K^{-1}C_1^2 Z_1 x^2, \\ \text{and } Y_1 &= \frac{1}{3\sqrt{2}}C_1 Y + \frac{1}{2}C_1^2 Z_1, \\ Z_1 &= Z - C_1^{-1}. \end{aligned} \right\} \quad (\text{C } 13)$$

We see from this that Y_1 , the axis of the butterfly that bisects the wings, denoted v by Thom (1975, pp. 68–73) and t_2 by Poston & Stewart (1976, p. 74), is tilted in the plane (Y , Z), not merely by the slope at B_1 of the original wavefront centred on O , but even when observed looking down the normal on to B_1 ; the tangent of the angle of tilt is $(3/2\sqrt{2})C_1 l_0$. If the drop size is approximately l_0 , the curvature of the wavefront C_1 has to be small compared with l_0^{-1} to satisfy the small slope approximation all over the drop, and the tilt is then small. However, if we are only interested, as in this appendix, in the local wavefront at B_1 , and if we take the z axis normal to the wavefront at B_1 , the slopes will always be small locally; there is then no reason to restrict the value of C_1 and the tilt of the butterfly need not be small.

REFERENCES

- Berry, M. V. 1976 Waves and Thom's theorem. *Adv. Phys.* **25** (1), 1–26.
 Berry, M. V. & Nye, J. F. 1977 Fine structure in caustic junctions. *Nature, Lond.* **267**, 34–6.
 Poston, T. & Stewart, I. N. 1976 *Taylor expansions and catastrophes*. London: Pitman.
 Thom, R. 1975 Structural stability and morphogenesis: an outline of a general theory of models. Reading, Massachusetts: W. A. Benjamin Inc.
 Trinkaus, H. & Drepper, F. 1977 On the analysis of diffraction catastrophes. *J. Phys. A: Math. Gen.* **10** (1), L11–16.